# Photoprotective Potential of Penta-O-Galloyl-β-D-Glucose by Targeting NF-κB and MAPK Signaling in UVB Radiation-Induced Human Dermal Fibroblasts and Mouse Skin

Byung-Hak Kim[1,2], Mi Sun Choi[3], Hyun Gyu Lee[4], Song-Hee Lee[1], Kum Hee Noh[1], Sunho Kwon[1], Ae Jin Jeong[1], Haeri Lee[1], Eun Hee Yi[1,5], Jung Youl Park[6], Jintae Lee[7], Eun Young Joo[3], and Sang-Kyu Ye[1,2,5,8,]*

Exposure of the skin to ultraviolet radiation can cause skin damage with various pathological changes including inflammation. In the present study, we identified the skin-protective activity of 1,2,3,4,6-penta-O-galloyl-β-D-glucose (pentagalloyl glucose, PGG) in ultraviolet B (UVB) radiation-induced human dermal fibroblasts and mouse skin. PGG exhibited antioxidant activity with regard to intracellular reactive oxygen species (ROS) generation as well as ROS and reactive nitrogen species (RNS) scavenging. Furthermore, PGG exhibited anti-inflammatory activity, inhibiting the activation of nuclear factor-kappaB (NF-κB) and mitogen-activated protein kinase (MAPK) signaling, resulting in inhibition of the expression of pro-inflammatory mediators. Topical application of PGG followed by chronic exposure to UVB radiation in the dorsal skin of hairless mice resulted in a significant decrease in the progression of inflammatory skin damages, leading to inhibited activation of NF-κB signaling and expression of pro-inflammatory mediators. The present study demonstrated that PGG protected from skin damage induced by UVB radiation, and thus, may be a potential candidate for the prevention of environmental stimuli-induced inflammatory skin damage.

[1]Department of Pharmacology, [2]Biomedical Science Project (BK21 PLUS), Seoul National University College of Medicine, Seoul 110-799, Korea, [3]Department of Herbal Biotechnology, Daegu Haany University, Gyeongsan 38610, Korea, [4]Department of Microbiology and Immunology, Yonsei University College of Medicine, Seoul 03722, Korea, [5]Ischemic/Hypoxic Disease Institute, Seoul National University College of Medicine, Seoul 110-799, Korea, [6]Industry-Academic Cooperation Foundation, Hanbat National University, Daejeon 305-719, Korea, [7]Department of Cosmeceutical Science, Daegu Haany University, Gyeongsan 38610, Korea, [8]Neuro-Immune Information Storage Network Research Center, Seoul National University College of Medicine, Seoul 110-799, Korea
*Correspondence: sangkyu@snu.ac.kr

## INTRODUCTION

Solar radiation is one of the most important environmental factors leading to skin damage. Ultraviolet (UV) light is one part of the spectrum of solar radiation that primarily affects the skin. The UV radiation is a part of the electromagnetic spectrum of solar radiation that can be divided into UVA, UVB, and UVC bands by wavelength. UVA has the longest wavelength, at 320-400 nm, and UVB covers the range of 290-320 nm. Both wavelengths have positive and negative health effects in humans. Small amounts of UV are essential for the synthesis of vitamin D; however, overexposure may result in acute and chronic health effects in the skin, eye, and immune system. Unlike UVA and UVB, with even shorter wavelength rays, most UVC, in the range of 200-290 nm, does not reach the Earth due to absorption by the ozone layer (Diffey, 1991; Yagura et al., 2011).

The skin is the outermost organ of the human body and is continually exposed to environmental stimuli such as solar radiation, which lead to oxidative stress and induce inflammation through increasing the generation of reactive oxygen species (ROS) and reactive nitrogen species (RNS). Repeated and chronic exposure to UV radiation induces photodamage in the skin, resulting in clinical, histological, and functional changes in the areas of habitually sun-exposed skin. UV radiation penetrates the superficial epidermal layers and dermis of the skin, resulting in an acute inflammatory response characterized by erythema and edema formation, infiltration of immune cells, and increased blood vessel formation (Alfadda and Sallam, 2012, Brieger et al., 2012; Ichihashi et al., 2003; Svobodova et al., 2006). UV radiation-induced skin damage is triggered via various signaling pathways such as receptor-initiated signaling, mitochondrial damage, protein oxidation, telomere-based DNA damage, and aryl hydrocarbon receptor (AhR) signaling (Klotz et al., 2001; Krutmann et al., 2012; Yaar and Gilchrest, 2007). During UV radiation, large amounts of ROS and RNS are produced and trigger multiple receptor-initiated signaling pathways

in dermal fibroblasts and keratinocytes. ROS- and/or RNS-mediated receptor activation mainly results in the activation of transcription factors such as nuclear factor-kappaB (NF-κB) and activator protein-1 (AP-1), initiating intracellular signaling events (Berneburg et al., 2000; Fisher et al., 1996; Lee et al., 2010). These activated transcription factors increase the synthesis of numerous pro-inflammatory mediators in fibroblasts and keratinocytes, exaggerating skin damage and inducing skin diseases, such as local inflammation, skin aging, pigmentation, and cancer (Farage et al., 2008; Gilchrest, 2013; Kohl et al., 2011; Uitto, 1997).

1,2,3,4,6-Penta-O-galloyl-β-D-glucose (PGG) is a naturally occurring polyphenolic compound that can be found in several medicinal herbs, such as *Rhus chinensis*, *Rhus typhina*, *Punica granatum*, *Paeonia lactiflora*, and *Paeonia suffruticosa* (Hofmann and Gross, 1990; Lee et al., 2003; Park et al., 2008; Yu et al., 2011). Several *in vitro* and *in vivo* studies have shown that PGG exhibits a wide range of biological activities (Zhang et al., 2009), suggesting possibilities in the therapy and prevention of several diseases. In the present study, we synthesized PGG chemically and found that it exhibited UVB radiation-induced skin protective activity. To assess this, we performed *in vitro* studies in human dermal fibroblasts and an *in vivo* study in a hairless mouse model with UVB radiation. PGG alleviated UVB radiation-induced skin damage in the hairless mouse model, and this activity was associated with its antioxidant and anti-inflammatory properties.

## MATERIALS AND METHODS

### Reagents and antibodies
Tannic acid and 2',7'-dichlorofluorescin diacetate (DCF-DA) were obtained from Sigma-Aldrich (USA). Antibodies specific for phospho-IκBα (Ser32/36), phospho-NF-κB p65 (Ser536), phospho-IKKα/β (Ser176/180), IKKβ, phospho-p38 (Thr180/Tyr 182), p38, phospho-ERK1/2 (Thr202/Tyr204), ERK1/2, phospho-JNK (Thr183/Tyr185), JNK, COX-2, ICAM-1, and GAPDH were obtained from Cell Signaling Technology (USA). Anti-IκBα and anti-NF-κB p65 antibodies were purchased from Santa Cruz Biotechnology (USA). Horseradish peroxidase (HRP)-conjugated anti-rabbit antibody was obtained from Life Technologies (USA). All of the other chemicals used were analytical grade and purchased from Sigma-Aldrich unless otherwise noted.

### Synthesis and purification of PGG
PGG was synthesized from tannic acid by a modification of Chen and Hagerman's method (Chen and Hagerman, 2004). Briefly, tannic acid (10.0 g) was dissolved in methanolysis solution (70% methanol 140 ml and 0.1 M acetate buffer 60 ml). The mixture was heated at 65°C for 16 h, and then adjusted to pH 6.0 by addition of 0.25 M NaOH. After removal of methanol, the reactant was resuspended in distilled water and partitioned into ethyl ether and aqueous layers following ethyl acetate. PGG was purified from the ethyl acetate fraction by high-performance liquid chromatography (HPLC) using a separation technology column (J'sphere ODS, 4 μm, 250 × 4.6 mm), and an acetonitrile-water gradient with 0.1% trifluoroacetic acid (TFA) to afford 300 mg of PGG. This was identified by reversed-phase HPLC and fast atom bombardment bass spectrometry (FAB-MS). PGG with a purity ≥ 97% was dissolved in dimethyl sulfoxide (DMSO) as a 10 mM stock solution, and kept at -20°C in aliquots.

### Cell culture and UVB radiation
Normal human dermal fibroblasts were obtained from Modern Cell & Tissue Technologies (Korea), and maintained in Dulbecco's Modified Eagle's Medium (DMEM) containing 10% fetal bovine serum (FBS) and 1% penicillin-streptomycin (Life Technologies) in a humidified atmosphere of 5% $CO_2$ and 95% air at 37°C. Cells pre-incubated with PGG for 1 h were washed with PBS and exposed to a 100 mJ/cm$^2$ UVB light with a 312 nm UVB light source (VL-6.LM, Vilber Lourmat, France). The UVB intensity was measured with a Waldmann UV meter (model 585100, Germany). After UVB radiation, the cells were washed with PBS, and replaced with PGG containing media for appropriate time periods.

### Cell viability assay
Cell viability was determined using EZ-CyTox Enhanced Cell Viability Assay Kit (Daeil Lab Service, Korea) containing the WST-1 reagent. Cells were treated with various concentrations of PGG or irradiated with various doses of UVB. After incubation for 24 h, assay reagent was added and absorbance of the soluble formazan was measured at 450 nm using a microplate reader (Molecular Devices, USA) after a reaction at 37°C, as previously described (Kim et al., 2013a; 2015).

### Measurement of ROS and superoxide production
UVB-irradiated cells were incubated for 6 h following incubation with PGG for 1 h in serum-free medium. ROS production was measured by staining with DCF-DA (10 μM), as previously described (Kim et al., 2013b). To examine superoxide production, cells pre-incubated with PGG for 30 min in the presence of lucigenin (25 μM) were irradiated with UVB, and superoxide production was immediately measured by lucigenin-dependent chemiluminescence, as previously described (Kim et al., 2013c).

### Measurement of superoxide- and peroxynitrite-scavenging activities
Superoxide radicals were produced by the non-enzymatic NADH/phenazine methosulfate (PMS) system and the radical scavenging activity was measured by reduction of nitroblue tetrazolium (NBT), as previously described (Kim et al., 2013c). The reaction mixtures containing PGG, NBT (100 μM), PMS (30 μM), and NADH (150 mM) in 50 mM phosphate buffer (pH 7.4) were incubated at 25°C for 5 min, and the absorbance was measured at 560 nm using a microplate reader. Peroxynitrite was synthesized from hydrogen peroxide and nitrite by a modification of Balavoine and Geletii's method (Balavoine and Geletii, 1999). The reaction mixture was prepared by mixing PGG (100 μl) and peroxynitrite (10 μl, 5 mM) in 35 mM phosphate buffer (pH 7.0). After quickly shaking the mixture, Pyrogallol Red (50 μM, 100 μl) was added, and the absorbance was measured at 542 nm using a microplate reader.

### Western blot analysis
Protein samples were resolved on SDS-PAGE and transferred onto polyvinylidene difluoride (PVDF) membranes (Life Technologies). Membranes were blocked for 1 h in a blocking buffer containing 5% skim milk in 25 mM Tris-HCl (pH 8.0), 150 mM NaCl, and 0.1% Tween 20, and incubated with specific primary antibodies for the target molecules overnight at 4°C. Blots were washed and incubated with horseradish peroxidase-conjugated secondary antibodies for 2 h at room temperature and the signals were detected using an ECL detection kit (SurModics Inc, USA).

### Semi-quantitative RT-PCR
Semi-quantitative RT-PCR was performed using an RNA PCR kit (Bioneer, Korea) according to the manufacturer's protocol.
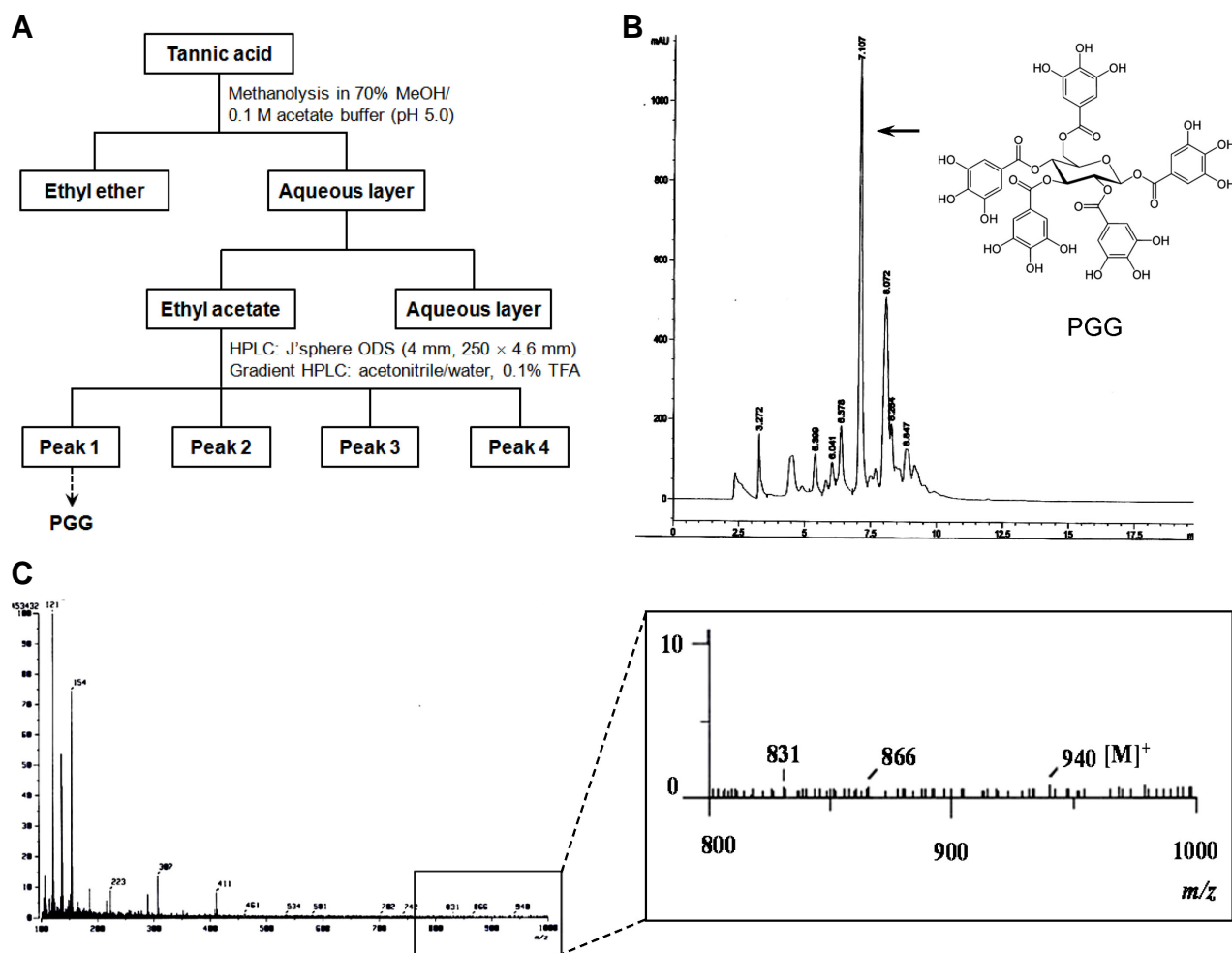
**Fig. 1.** Synthetic scheme and chromatogram of PGG. (A) PGG was synthesized from tannic acid by a methanolysis reaction. (B) HPLC chromatogram with chemical structure of PGG. PGG is composed of five galloyl groups with a glucose at its core. (C) FAB-MS chromatogram of PGG.

Briefly, total RNA was reverse-transcribed at 42°C for 1 h and PCR was performed 25 cycles at 94°C for 30 s, 58°C for 60 s, and 72°C for 60 s, with a final cycle at 72°C for 5 min. The primer sequences were: forward 5'-CCGAGGTGTATGTAT GAGTGTG-3' and reverse 5'-CAGGAGGAAGGGCTCTAGT ATAA-3' for COX-2 (NM_000963, 338 bp); forward 5'-GG CCACTGAAGAACCCATATTA-3' and reverse 5'-CTGTCTC CCATTAGACCACAAG-3' for IL-6 (AF372214, 323 bp); for-ward 5'-GAGCCGAATGGGACGTAAATA-3' and reverse 5'-CTCTCCATCAGAAGTGGGAATG-3' for IL-8 (AF385628, 317 bp); forward 5'-CTTGTTCCTCAGCCTCTTCTC-3' and reverse 5'-TTCTCTCTCATCCCTCCCTATC-3' for TNF-α (X02910, 215 bp); forward 5'-CCTTGTCCTCTTGTCCTGTTT-3' and reverse 5'-TGTGGTGTTGTGAGCCTATG-3' for ICAM-1 (NM_000201, 306 bp), and forward 5'-GGAAATCGTGCGTGACATTAAG-3' and reverse 5'-TAGTCCGCCTAGA AGCATTTG-3' for β-actin (NM_001101, 519 bp). The PCR products were resolved on agarose gels with DNA SafeStain (Lamda Biotech, USA) by electrophoresis.

**NF-κB reporter assay**

Cells were transfected with the NF-κB-luciferase construct and phRL-TK vector (Promega, USA), as previously described (Kim et al., 2011) using Lipofectamine LTX and PLUS reagent (Life Technologies). After 24 h, cells pre-incubated with PGG for 1 h were irradiated with UVB and further incubated for 24 h. NF-κB luciferase activity was measured using a Dual-Glo luciferase assay system (Promega) and the firefly luciferase activity was normalized to that of *Renilla* luciferase.

**Immunofluorescence staining**

UVB-irradiated cells were incubated for 6 h following pre-incubation with PGG for 1 h. Cells were fixed in 4% formalde-hyde, permeabilized with 0.1% Triton X-100 in PBS (pH 7.4), and blocked in PBS containing 10% goat serum, 0.3 M glycine, 1% BSA, and 0.1% Tween 20 for 2 h at room temperature. For immunostaining, the cells were incubated with anti-NF-κB p65 antibody at 4°C in PBS containing 1% BSA and 0.1% Tween 20 overnight, after which they were washed, and incubated with Alexa Fluor 568 anti-rabbit IgG antibody (Molecular Probes, USA) at room temperature for 1 h. The signals were imaged using an inverted fluorescence microscope (Carl Zeiss, Germany), and nuclei were counterstained with 4',6-diamidino-2-phenylindole (DAPI).
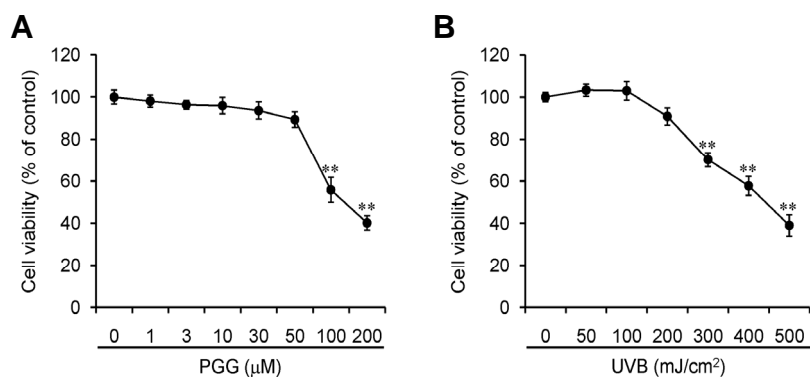
**Fig. 2.** Cell viability assays. Human dermal fibroblasts were incubated with various concentrations of PGG (A) for 24 h or irradiated with various doses of UVB and cultured for 24 h (B). Cell viability was measured with the WST-1 reagent, and results are shown as the means ± SD of three independent experiments ($n$ = 3). **$p$ < 0.005 compared to vehicle-treated group.

## Animal study

All of the animal experiments were reviewed and approved by the Institutional Animal Care and Use Committee (IACUC) of the Seoul National University College of Medicine. Male hairless mice (SKH:HR-1) at 6 weeks old were obtained from Central Lab. Animal Inc. (Korea). Mice (each group, $n$ = 10) were exposed to a dose of UVB irradiation (Sankyo Denki sunlamps, G9T5E, 290-320 nm, Japan) three times per week for 10 weeks on the dorsal skin. A regimen of progressive UVB exposure was used: starting at 1 week with 100 mJ/cm$^2$, which was increased weekly by 100 mJ/cm$^2$ until 4 weeks. Then, UVB irradiation exposure was 400 mJ/cm$^2$ over the next 6 weeks. Samples were applied topically with a vehicle [propylene glycol:ethanol = 7:3 (v/v)] or 10 mg/kg PGG following UVB irradiation. The PGG concentration was fixed at ~10 μM based on the results of an *in vitro* study.

## Histological analysis

Tissue specimens were obtained 24 h after final UVB irradiation. The specimens were fixed in 4% paraformaldehyde in PBS for 24 h, washed with tap water, dehydrated with grade ethanols, and then embedded in paraffin wax. The paraffin wax blocks were cut in 4 μm sections, mounted on glass slides, dewaxed, rehydrated through graded ethanols, and then stained with hematoxylin and eosin (H&E). Analyses were performed using a light microscope (Olympus, Japan).

## Statistical analysis

Data are presented as means ± standard deviation (SD) of three independent experiments ($n$ = 3). Statistical differences were determined using one-way ANOVA followed by Dunnett's multiple comparison tests. Differences were considered statistically significant at $p$ < 0.05.

## RESULTS

### Synthesis and purification of PGG

PGG is composed of five galloyl groups with a glucose at its core, and can be synthesized by several chemical reactions: a Steglich esterification of glucose with gallic acids (Khanbabaee and Lötzerich, 1997), a radio-labeled synthesis from $^{14}$C-glucose (Chen et al., 2003), and an anomeric-selective synthesis using anomerically pure glucose (Binkley et al., 2009). Here, we synthesized PGG from tannic acid (10.0 g) by a methanolysis reaction (Fig. 1A) by modification of Chen and Hagerman's method (Chen and Hagerman, 2004), as described in the Materials and Methods. The ethyl acetate layer contained large amounts of PGG (300 mg). The synthesized PGG was identified and purified by HPLC using a separation technology col-

umn and FAB-MS (Figs. 1B and 1C).

Before examining the biological activities of PGG, we first determined its cytotoxic activity by incubating human dermal fibroblasts with various concentrations of PGG or by exposing them to various dosages of UVB irradiation. PGG exhibited weak to no cytotoxic activity *in vitro* at concentrations of up to 50 μM (Fig. 2A). UVB irradiation also exhibited no cytotoxic activity in the cells up to 200 mJ/cm$^2$ (Fig. 2B). Thus, we used PGG below 50 μM and 200 mJ/cm$^2$ UVB irradiation in the *in vitro* experiments to avoid the possibility of cytotoxic effects.

### PGG exhibits antioxidant and ROS-scavenging activities

Large amounts of ROS and RNS were generated during UVB irradiation, and many naturally occurring polyphenolic compounds including tannic acid possess antioxidant activity (Pandey and Rizvi, 2009; Svobodová et al., 2003). To determine whether the synthesized polyphenolic compound PGG had biological activity, we first examined its antioxidant activity by measuring the effects on intracellular ROS and superoxide generation as well as ROS- and RNS-scavenging activities. Intracellular ROS generation was measured with confocal microscopy following staining with DCF-DA. Generation was negligible in vehicle-treated human dermal fibroblasts, whereas this was increased markedly by UVB irradiation. PGG effectively inhibited UVB radiation-induced intracellular ROS generation in the cells (Fig. 3A). Excessive intracellular ROS generation is primarily mediated by the NADPH oxidase complex, which is associated with inflammatory responses and disease pathogenesis (Fu et al., 2014; Kong et al., 2010). Thus, we next investigated whether PGG could affect NADPH oxidase-dependent superoxide production by measuring lucigenin-dependent chemiluminescence. Treatment with vehicle or PGG alone did not affect superoxide production in quiescent human dermal fibroblasts. However, the production was increased markedly by UVB irradiation in the cells, and PGG effectively inhibited this production in a concentration-dependent manner (Fig. 3B).

We further examined ROS- and RNS-scavenging activities of PGG by non-enzymatic assays. Superoxide radicals were produced in the presence of PMS and NADH by reaction with oxygen in the air, and peroxynitrite was synthesized by reaction with hydrogen peroxide and nitrite, as described in the "Materials and Methods". PGG exhibited effective superoxide radical-scavenging activity in a concentration-dependent manner (Fig. 3C), while this compound exhibited moderate peroxynitrite-scavenging activity (Fig. 3D). These data indicate that the synthesized PGG had biological activities, possessing antioxidant activity as well as ROS- and RNS-scavenging activities.
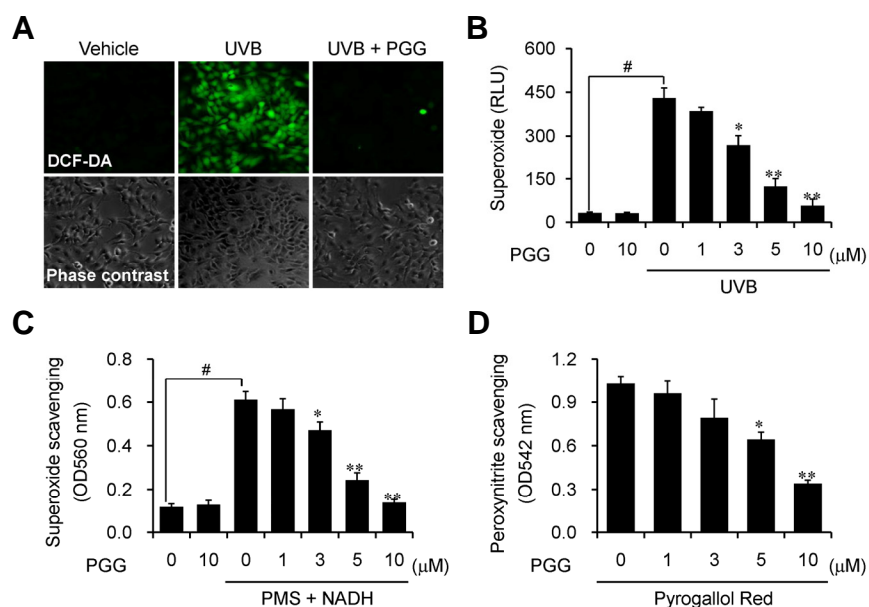
**Fig. 3.** PGG exhibits antioxidant activities. (A) Human dermal fibroblasts pre-incubated with vehicle or PGG (10 μM) for 1 h were irradiated with UVB (100 mJ/cm$^2$), and were stained with DCF-DA (10 μM) for 30 min. Intracellular ROS production was analyzed by fluorescence microscopy. (B) Human dermal fibroblasts were pre-treated with vehicle or PGG for 30 min, irradiated with UVB (100 mJ/cm$^2$), and superoxide anion production was measured by chemiluminescence. (C) Superoxide anion was produced by the NADH/PMS/NBT system and the scavenging activity was measured as absorbance at 560 nm using a microplate reader. Results are shown as the means ± SD of three independent experiments ($n$ = 3). #$p$ < 0.005 compared to vehicle-treated group; *$p$ < 0.05 and **$p$ < 0.005 compared to UVB-irradiated or NADH/PMS-containing group. (D) Peroxynitrite was synthesized by reac tion with hydrogen peroxide and nitrite and the scavenging activity was measured at 542 nm using a microplate reader following addition with Pyrogallol Red (50 μM). Results are shown as the means ± SD of three independent experiments ($n$ = 3). *$p$ < 0.05 and **$p$ < 0.005 compared to vehicle-treated group.

## PGG inhibits UVB radiation-induced NF-κB signaling

Excessive ROS generation by UVB irradiation-mediated NADPH oxidase complex modulates Toll-like receptor (TLR) signal transduction at multiple levels and subsequently induces inflammatory responses and disease pathogenesis via activation of signaling cascades, including nuclear factor- kappaB (NF-κB) (Fan et al., 2003; Liu et al., 2009; Park et al., 2006; Siomek,

2012). Several studies have reported an anti-inflammatory activity of PGG through inhibiting NF-κB signaling in different cell lines (Jang et al., 2013; Oh et al., 2004; Pan et al., 2000). Our results are consistent with previous reports. PGG effectively inhibited phosphorylation and degradation of IκBα, as well as phosphorylation of NF-κB and IKKα/β proteins in UVB radiation-induced human dermal fibroblasts (Figs. 4A and 4B).
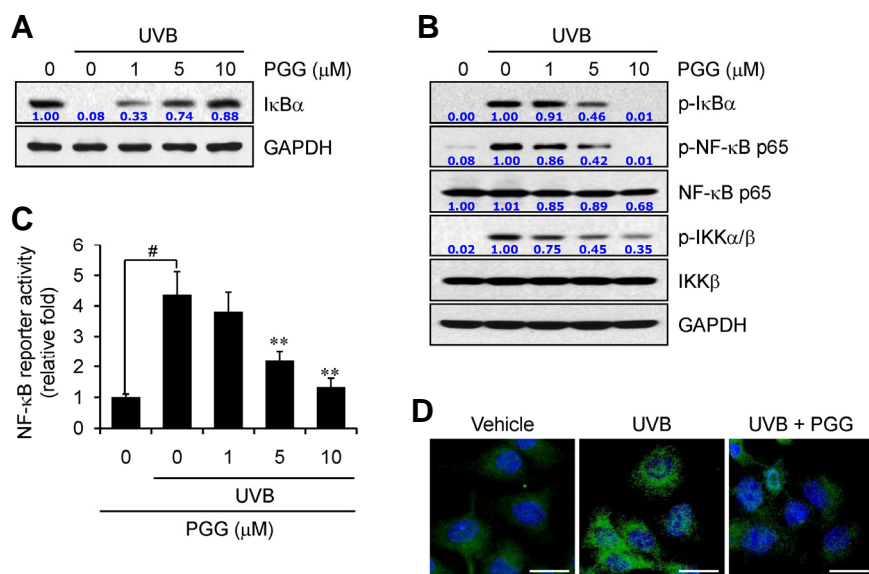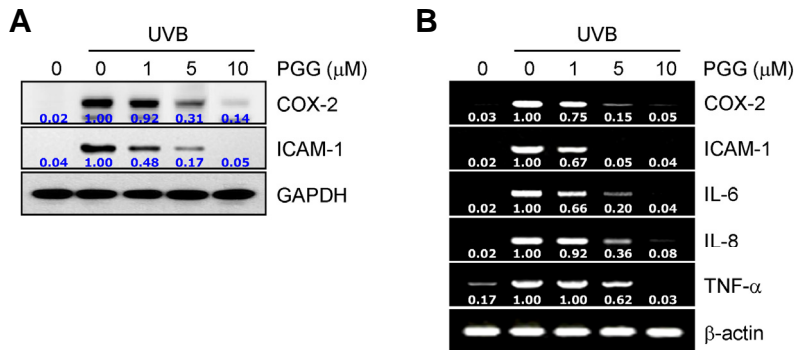


**Fig. 4.** PGG inhibits NF-κB signaling. (A, B) Human dermal fibroblasts were pre-incubated with vehicle or PGG for 1 h, irradiated with UVB (100 mJ/cm$^2$), and further incubated for 6 h. Western blot analysis was performed against the indicated target molecules. GAPDH served as a loading control. Data are representative of one of three independent experiments with similar results ($n$ = 3). (C) Human dermal fibroblasts were transfected with the NF-κB-luciferase construct and phRL-TK vector. After 24 h, cells pre-incubated with PGG for 1 h were irradiated with UVB (100 mJ/cm$^2$) and further incubated for 24 h. NF-κB luciferase activity was measured and the firefly luciferase activity was normalized to that of *Renilla* luciferase. Data are presented as the means ± SD of three independent experiments ($n$ = 3). #$p$ < 0.005 compared to vehicle-treated group; **$p$ < 0.005 compared to UVB-irradiated group. (D) Pre-incubated human dermal fibroblasts for 1 h were irradiated with UVB (100 mJ/cm$^2$), and further incubated for 6 h. Nuclear translocation of NF-κB p65 (green) was analyzed by immunohistochemical analysis, as described in the "Materials and Methods". Nuclei were counterstained with DAPI (blue). Scale bar = 50 μm.
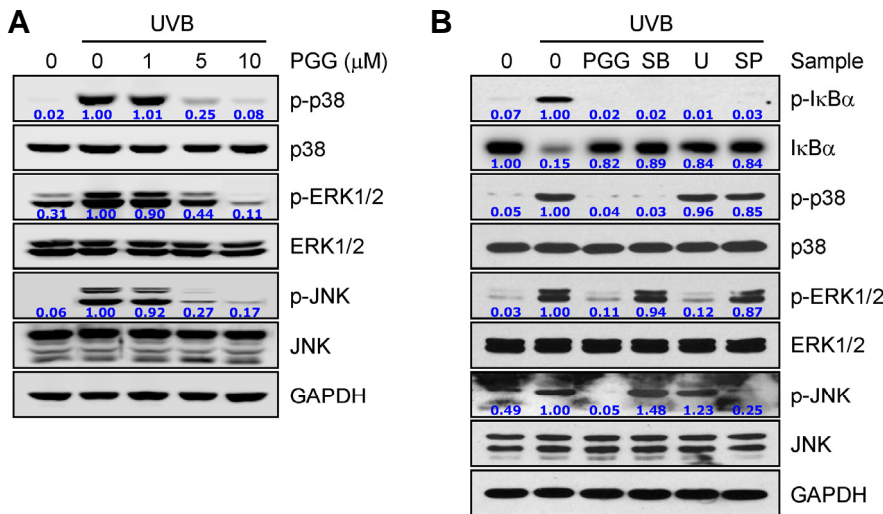
**Fig. 5.** PGG inhibits MAP kinase signaling. (A) Human dermal fibroblasts were pre-incubated with vehicle or PGG for 1 h, irradiated with UVB (100 mJ/cm$^2$), and further incubated for 30 min. (B) Cells were irradiated with UVB (100 mJ/cm$^2$) and further incubated for 6 h, followed by incubation for 16 h in the presence of each compound. Western blot analysis was performed against the indicated target molecules. GAPDH served as a loading control. Data are representative of one of three independent experiments with similar results ($n$ = 3). PGG (10 μM); SB, SB203580 (40 μM); U, U0126 (40 μM), SP, SP600125 (40 μM).



**Fig. 6.** PGG inhibits the expression of pro-inflammatory mediators. Human dermal fibroblasts were pre-incubated with vehicle or PGG for 1 h, irradiated with UVB (100 mJ/cm$^2$), and further incubated for 24 h or 6 h, respectively. Western blot (A) and RT-PCR (B) analyses were performed. GAPDH and β-actin served as loading controls. Data are representative of one of three independent experiments with similar results ($n$ = 3).

Next, we examined NF-κB-dependent reporter activity by measuring luciferase activity followed by transfection with the NF-κB-luciferase construct in human dermal fibroblasts. Luciferase activity increased after UVB irradiation, while incubation with PGG effectively inhibited activity in a concentration-dependent manner (Fig. 4C). Consistent results were observed by immunofluorescence staining of NF-κB. Large amounts of immunostained NF-κB p65 (green) were observed in the nucleus by UVB irradiation, compared with the vehicle-treated group, indicating that activated NF-κB p65 was translocated into the nucleus, where this translocation was effectively inhibited in the presence of PGG (Fig. 4D). These data clearly indicates that the PGG synthesized was a potent inhibitor of UVB radiation-induced NF-κB signaling and may suppress UVB radiation-induced inflammatory responses in the skin.

**PGG inhibits UVB radiation-induced MAP kinases signaling**
UVB radiation-induced photoproduced ROS also activate a wide range of signaling pathways including MAP kinases in human dermal fibroblasts (Jang et al., 2013). MAP kinases, such as p-38 MAPK, extracellular signal-regulated kinase (ERK), and stress-activated protein kinase (SAPK)/c-Jun N-terminal kinase (JNK), also play key roles in inflammatory signaling by regulation of NF-κB signaling in various cell types, but also regulate proliferation, differentiation, and survival in mammalian cells (Matsumoto et al., 2000; Wang et al., 2009). Thus, next we examined whether PGG could regulate these signaling pathways. The activation of MAP kinases, p38, ERK1/2, and

JNK, was increased by UVB irradiation in human dermal fibroblasts, whereas activation of these kinases was effectively inhibited by PGG treatment in a concentration-dependent manner (Fig. 5A). In addition, blocking of the MAPK signaling by specific inhibitor effectively inhibited degradation and phosphorylation of the IκBα protein (Fig. 5B), indicating that PGG-mediated inhibition of the MAPK signaling may be an important upstream to regulate NF-κB signaling in UVB radiation-induced human dermal fibroblasts. These data suggest that PGG may regulate inflammatory responses as well as cell proliferation, differentiation, and survival mediated by excessive photoproduced ROS from UVB irradiation in the skin.

**PGG inhibits UVB radiation-induced the expression of pro-inflammatory mediators**
UVB radiation-induced photoproduced ROS initiate multiple signal transduction processes and induce inflammatory responses by upregulating the expression of pro-inflammatory mediators in the skin (Bickers and Athar, 2006; Wagener et al., 2013). To investigate whether PGG could exhibit skin-protective activity in connection with photodamage-mediated inflammation from UVB irradiation, we measured the expression of pro-inflammatory mediators in human dermal fibroblasts. Western blotting data showed that UVB irradiation upregulated the expression of COX-2 and ICAM-1 proteins, whereas PGG treatment effectively suppressed their expression (Fig. 6A). We found similar results in the mRNA levels of these proteins as well as the pro-inflammatory cytokines IL-6, IL-8, and TNF-α. The mRNA levels of these pro-inflammatory mediators were
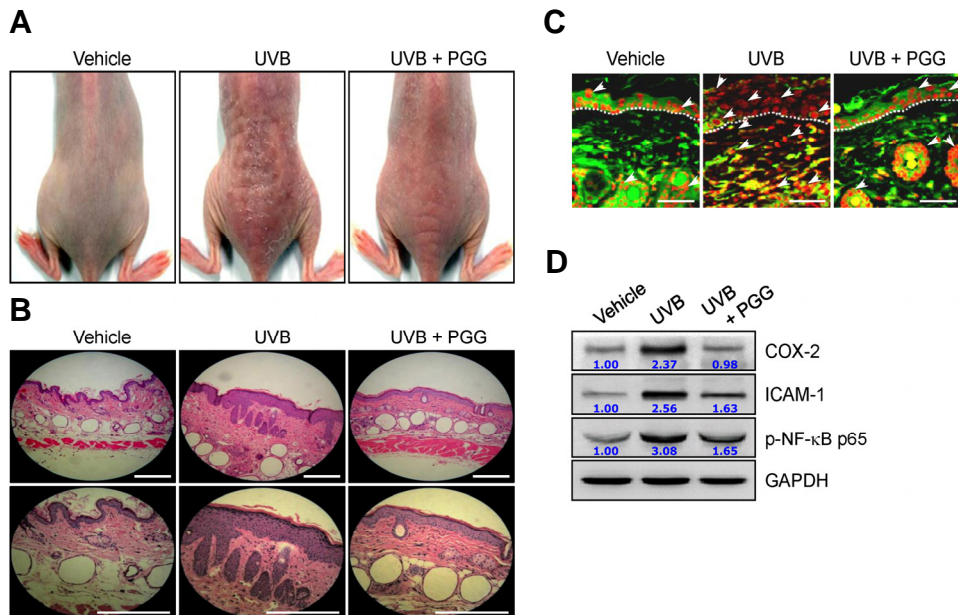
**Fig. 7.** PGG protects against photodamage in mouse skin. SKH:HR-1 hairless mice were irradiated with UVB three times per week for 10 weeks as described in the Materials and Methods and PGG (10 mg/kg) was applied topically 1 h after UVB irradiation. (A) The macroscopic images of mouse backs are represented. (B-D) The sections of skin specimens were stained with H&E (B, scale bar = 100 μm), immunohistochemical staining using an active NF-κB p65 antibody (C, dark red, scale bar = 50 μm), and Western blot analysis (D). The white arrows indicate active NF-κB p65 and dotted lines indicate the boundary of epidermis and dermis. A representative picture is shown from each group (n = 10).

increased in UVB radiation-induced human dermal fibroblasts, whereas the levels were effectively decreased in the presence of PGG in a concentration-dependent manner in the cells (Fig. 6B). These data suggest that PGG can protect against UVB radiation-induced photodamage in the skin through suppression of the expression of pro-inflammatory mediators.

## PGG alleviates UVB radiation-induced inflammatory skin damage in mouse skin

Because chronic exposure to UVB irradiation increases ROS production and leads to inflammatory responses in the skin, we performed an *in vitro* experiment with chronic exposure to UVB in the hairless mouse to assess whether PGG could suppress UVB radiation-induced skin damage. PGG was applied topically to the dorsal trunk of SKH:HR-1 hairless mice followed by UVB irradiation, three times per week for 6 weeks. Macroscopic photos showed that the skin was much drier and paler, and increased fine wrinkles were seen in UVB radiation-induced mice versus the vehicle-treated mice, whereas these superficial changes were reduced markedly by PGG treatment (Fig. 7A).

Histological analysis with H&E staining of the dorsal skin showed that UVB irradiation resulted in increased inflammatory responses such as increased skin thickness, epidermal hyperplasia with enlarged sebaceous glands, hyperkeratosis, and increased inflammatory cell infiltration in the skin of mice, compared with vehicle-treated mice, whereas the topical application of PGG reduced these morphological changes, indicating photoprotective activity of PGG in the skin (Fig. 7B). We also observed similar results with *in vitro* experiments on NF-κB signaling and the levels of pro-inflammatory mediators. The activation of NF-κB p65 and the levels of COX-2 and ICAM-1 were increased in the skin of the UVB radiation-induced group, compared with the vehicle-treated group, while this activation and levels were effectively suppressed by topical application with PGG on the skin (Figs. 7C and 7D). Overall, these results are consistent with the UVB radiation-induced human dermal fibroblasts, and suggest that PGG exhibits anti-inflammatory and skin-protective activities against UVB irradiation.

## DISCUSSION

Solar radiation is composed of infrared (IR), visible, and UV light. Repeated and chronic exposure of skin areas to solar radiation induces skin damage, including inflammation. From the whole spectrum of solar radiation, the harmful biological effects of UV irradiation have become serious issues, and have been defined over past decades. In the present study, we synthesized PGG and investigated its skin-protective activity in UVB radiation-induced human dermal fibroblasts and mice. The polyphenolic compound PGG consists of a glucose core with five galloyl groups, and is the common immediate precursor of both gallotannins and ellagitannins (Niemetz and Gross, 2005). Several synthetic methods for PGG are known, such as the esterification of glucose with gallic acid, radiolabeled synthesis from ^{14}C-glucose, and an anomeric-selective synthesis using anomerically pure glucose (Binkley et al., 2009; Chen et al., 2003; Khanbabaee and Lötzerich, 1997). Here, we synthesized PGG from tannic acid by a methanolysis reaction using a modification of Chen and Hagerman's method (Chen and Hagerman, 2004), and purified it using HPLC and FAB-MS, although it can also be found in several medicinal herbs such as *Punica granatum* (pomegranate), *Rhus typhina* (staghorn sumac), *Rhus chinensis* (gallnut), *Paeonia lactiflora* (peony), *Paeonia suffruticosa* (tree peony), and *Elaeocarpus sylvestris* (Hofmann and Gross, 1990; Lee et al., 2003; Park et al., 2008; Yu et al., 2011). Our synthetic procedure was very simple and economical compared with other methods, and can produce larger amounts of PGG than isolation from medicinal herbs. The yield was 3 %; we obtained 300 mg PGG from 10.0 g tannic acid.

Solar radiation is the main source of UV radiation in the environment, of which about 95% is UVA and ~5% is UVB, whereas UVC is almost completely absorbed by the ozone layer in the upper part of the stratosphere (Hockberger, 2002). UV radiation is a primary external stress due to its strong potential for the production of ROS and RNS. ROS- and/or RNS-mediated oxidative stress disrupt endogenous antioxidant systems, and eventually result in inflammation and ECM remodeling in the

skin. In addition, highly reactive oxygen and nitrogen intermediates can readily react with various biological macromolecules, such as DNA, proteins and lipids to cause mutations, peroxidation of membrane lipids, and protein destruction, repectively. Eventually, these lesions can, in turn, lead to various degenerative processes, such as skin aging, pigmentation, and carcinogenesis (Farage et al., 2008; Gilchrest, 2013; Kohl et al., 2011; Uitto, 1997). Thus, restoration of antioxidant systems and/or antioxidant therapy may have the potential to protect against UV radiation-induced pathogenic processes. Our results demonstrated that the PGG synthesized exhibited effective antioxidant activity, which was observed by the inhibition of intracellular ROS and superoxide production in UVB radiation-induced human dermal fibroblast. We further observed that PGG has ROS- and RNS-scavenging activities. ROS and RNS were generated by the non-enzymatic NADH/PMS and $H_2O_2/NO_2$ systems *in vitro*, respectively. PGG has effective superoxide anion-scavenging activity, whereas the peroxynitrite anion was scavenged moderately.

Photoproduced ROS in UVB irradiation are one of the major factors known to induce inflammatory responses by altering ECM components through activation of multiple signaling pathways, such as NF-κB, AP-1, JAK/STAT, HIF-1α, and MAPK (Berneburg et al., 2000; Fisher et al., 2000; Jang et al., 2013; Lee et al., 2010). Application of antioxidants prevents UVB radiation-induced skin damage in dermal fibroblast and keratinocytes as well as in hairless mouse skin (Bissett et al., 1990; Kim et al., 2001). Our *in vitro* and *in vivo* data demonstrated that PGG effectively inhibited the activation of the NF-κB and MAPKs signaling pathways in UVB radiation-induced human dermal fibroblasts and mouse skin, leading to inhibition of the expression of pro-inflammatory mediators such as COX-2, ICAM-1, IL-6, IL-8, and TNF-α, suggesting that the anti-inflammatory activity of PGG may be associated with antioxidant, ROS- and RNS-scavenging activities.

In summary, we synthesized chemically and demonstrated the skin-protective activity of PGG in UVB radiation-induced human dermal fibroblasts and mouse skin. PGG exhibited effective antioxidant and ROS-scavenging activities, resulting in the inhibition of NF-κB and MAPKs signaling. As results, PGG exhibited an anti-inflammatory effect by downregulating the expression of the pro-inflammatory mediators both *in vitro* and *in vivo*. Our results suggest that PGG is a potential candidate for the prevention of UVB radiation-induced skin damage.

## REFERENCES

Alfadda, A.A., and Sallam, R.M. (2012). Reactive oxygen species in health and disease. J. Biomed. Biotechnol. *2012*, 936486.

Balavoine, G.G., and Geletii, Y.V. (1999). Peroxynitrite scavenging by different antioxidants. Part I: convenient assay. Nitric Oxide *3*, 40-54.

Berneburg, M., Plettenberg, H., and Krutmann, J. (2000). Photoaging of human skin. Photodermatol. Photoimmunol. Photomed. *16*, 239-244.

Bickers, DR, and Athar M. (2006). Oxidative stress in the pathogenesis of skin disease. J. Invest. Dermatol. *126*, 2565-2575.

Binkley, R.C., Ziepfel, J.C., and Himmeldirk, K.B. (2009). Anomeric selectivity in the synthesis of galloyl esters of D-glucose. Carbohydr. Res. *344*, 237-239.

Bissett, D.L., Chatterjee, R., and Hannon, D.P. (1990). Photoprotective effect of superoxide-scavenging antioxidants against ultraviolet radiation-induced chronic skin damage in the hairless mouse. Photodermatol. Photoimmunol. Photomed. *7*, 56-62.

Brieger, K., Schiavone, S., Miller, F.J. Jr., and Krause, K.H. (2012). Reactive oxygen species: from health to disease. Swiss Med. Wkly *142*, w13659.

Chen, Y., and Hagerman, A.E. (2004). Characterization of soluble non-covalent complexes between bovine serum albumin and beta-1,2,3,4,6-penta-O-galloyl-D-glucopyranose by MALDI-TOF MS. J. Agric. Food Chem. *52*, 4008-4011.

Chen, Y., Hagerman, A.E., and Minto, R. (2003). Preparation of 1,2,3,4,6-penta-O-galloyl-[U-$^{14}$C]-D-glucopyranose. J. Labelled Compd. Rad. *46*, 99-105.

Diffey, B.L. (1991). Solar ultraviolet radiation effects on biological systems. Phys. Med. Biol. *36*, 299-328.

Fan, J., Frey, M.S., and Malik, A.B. (2003). TLR4 signaling induces TLR2 expression in endothelial cells via neutrophil NADPH oxidase. J. Clin. Invest. *112*, 1234-1243.

Farage, M.A., Miller, K.W., Elsner, P., and Maibach, H.I. (2008). Intrinsic and extrinsic factors in skin ageing: a review. Int. J. Cosmet. Sci. *30*, 87-95.

Fisher, G.J., Datta, S.C., Talwar, H.S., Wang, Z.Q., Varani, J., Kang, S., and Voorhees, J.J. (1996). Molecular basis of sun-induced premature skin ageing and retinoid antagonism. Nature *379*, 335-339.

Fisher, G.J., Datta, S., Wang, Z., Li, X.Y., Quan, T., Chung, J.H., Kang, S., and Voorhees, J.J. (2000). c-Jun-dependent inhibition of cutaneous procollagen transcription following ultraviolet irradiation is reversed by all-trans retinoic acid. J. Clin. Invest. *106*, 663-670.

Fu, X.J., Peng, Y.B., Hu, Y.P., Shi, Y.Z., Yao, M., and Zhang, X. (2014). NADPH oxidase 1 and its derived reactive oxygen species mediated tissue injury and repair. Oxid. Med. Cell. Longev. *2014*, 282854.

Gilchrest, BA. (2013). Photoaging. J. Invest. Dermatol. *133*, E2-E6.

Hofmann, A.S., and Gross, G.G. (1990). Biosynthesis of gallotannins: formation of polygalloylglucoses by enzymatic acylation of 1,2,3,4,6-penta-O-galloylglucose. Arch. Biochem. Biophys. *283*, 530-532.

Hockberger, P.E. (2002). A history of ultraviolet photobiology for humans, animals and microorganisms. Photochem. Photobiol. *76*, 561-579.

Ichihashi, M., Ueda, M., Budiyanto, A., Bito, T., Oka, M., Fukunaga, M., Tsuru, K., and Horikawa, T. (2003). UV-induced skin damage. Toxicology *189*, 21-39.

Jang, S.E., Hyam, S.R., Jeong, J.J., Han, M.J., and Kim, D.H. (2013). Penta-O-galloyl-β-D-glucose ameliorates inflammation by inhibiting MyD88/NF-κB and MyD88/MAPK signalling pathways. Br. J. Pharmacol. *170*, 1078-1091.

Khanbabaee, K., and Lötzerich, K. (1997). Efficient total synthesis of the natural products 2,3,4,6-tetra-O-galloyl-d-glucopyranose, 1,2,3,4,6-penta-O-galloyl-beta-D-glucopyranose and the unnatural 1,2,3,4,6-penta-O-galloyl-alpha-D-glucopyranose. Tetrahedron *53*, 10725-10732.

Kim, J., Hwang, J.S., Cho, Y.K., Han, Y., Jeon, Y.J., and Yang, K.H. (2001). Protective effects of (-)-epigallocatechin-3-gallate on UVA- and UVB-induced skin damage. Skin Pharmacol. Appl. Skin Physiol. *14*, 11-19.

Kim, Y., Kim, B.H., Lee, H., Jeon, B., Lee, Y.S., Kwon, M.J., Kim, T.Y. (2011). Regulation of skin inflammation and angiogenesis by EC-SOD via HIF-1α and NF-κB pathways. Free Radic. Biol. Med. *51*, 1985-1995.

Kim, B.H., Won, C., Lee, Y.H., Choi, J.S., Noh, K.H., Han, S., Lee, H., Lee, C.S., Lee, D.S., Ye, S.K., et al. (2013a). Sophoraflavanone G induces apoptosis of human cancer cells by targeting upstream signals of STATs. Biochem. Pharmacol. *86*, 950-959.

Kim, B.H., Na, K.M., Oh, I., Song, I.H., Lee, Y.S., Shin, J., and Kim, T.Y. (2013b). Kurarinone regulates immune responses through regulation of the JAK/STAT and TCR-mediated signaling pathways. Biochem. Pharmacol. *85*, 1134-1144.

Kim, B.H., Choi, J.S., Yi, E.H., Lee, J.K., Won, C., Ye, S.K., and Kim, M.H. (2013c). Relative antioxidant activities of quercetin and its

structurally related substances and their effects on NF-κB/CRE/AP-1 signaling in murine macrophages. Mol. Cells 35, 410-420.

Kim, B.H., Han, S., Lee, H., Park, C.H., Chung, Y.M., Shin, K., Lee, H.G., and Ye, S.K. (2015). Metformin enhances the anti-adipogenic effects of atorvastatin via modulation of STAT3 and TGF-β/Smad3 signaling. Biochem. Biophys. Res. Commun. 456, 173-178.

Klotz, L.O., Holbrook, N.J., and Sies, H. (2001). UVA and singlet oxygen as inducers of cutaneous signaling events. Curr. Probl. Dermatol. 29, 95-113.

Kohl, E., Steinbauer, J., Landthaler, M., and Szeimies, R.M. (2011). Skin ageing. J. Eur. Acad. Dermatol. Venereol. 25, 873-884.

Kong X., Thimmulappa, R., Kombairaju, P., and Biswal, S. (2010). NADPH oxidase-dependent reactive oxygen species mediate amplified TLR4 signaling and sepsis-induced motality in Nrf2-deficient mice. J. Immunol. 185, 569-577.

Krutmann, J., Morita, A., and Chung, J.H. (2012). Sun exposure: what molecular photodermatology tells us about its good and bad sides. J. Invest. Dermatol. 132, 976-984.

Lee, S.J., Lee, I.S., and Mar, W. (2003). Inhibition of inducible nitric oxide synthase and cyclooxygenase-2 activity by 1,2,3,4,6-penta-O-galloyl-beta-D-glucose in murine macrophage cells. Arch. Pharm. Res. 26, 832-839.

Lee, E.J., Jeon, M.S., Kim, B.D., Kim, J.H., Kwon, Y.G., Lee, H., Lee, Y.S., Yang, J.H., and Kim, T.Y. (2010). Capsiate inhibits ultraviolet B-induced skin inflammation by inhibiting Src family kinases and epidermal growth factor receptor signaling. Free Radic. Biol. Med. 48, 1133-1143.

Liu, X., Shi, S., Ye, J., Liu, L., Sun, M., and Wang, C. (2009). Effect of polypeptide from Chlamys farreri on UVB-induced ROS/NF-kappaB/COX-2 activation and apoptosis in HaCaT cells. J. Photochem. Photobiol. B. 96, 109-116.

Matsumoto, M., Sudo, T., Saito, T., Osada, H., and Tsujimoto, M. (2000). Involvement of p38 mitogen-activated protein kinase signaling pathway in osteoclstogenesis mediated by receptor activator of NF-kappa B ligand (RANKL). J. Biol. Chem. 275, 31155-31161.

Niemetz, R., and Gross, G.G. (2005). Enzymology of gallotannin and ellagitannin biosynthesis. Phytochemistry 66, 2001-2011.

Oh, G.S., Pae, H.O., Choi, B.M., Lee, H.S., Kim, I.K., Yun, Y.G., Kim, J.D., and Chung, H.T. (2004). Penta-O-galloyl-beta-D-glucose inhibits phorbol myristate acetate-induced interleukin-8 gene expression in human monocytic U937 cells through its inactivation of nuclear factor-kappaB. Int. Immunopharmacol. 4, 377-386.

Pan, M.H., Lin-Shiau, S.Y., Ho, C.T., Lin, J.H., and Lin, J.K. (2000). Suppression of lipopolysaccharide-induced nuclear factor-kappaB activity by theaflavin-3,3'-digallate from black tea and other polyphenols through down-regulation of IkappaB kinase activity in macrophages. Biochem. Pharmacol. 59, 357-367.

Pandey, K.B., and Rizvi, S.I. (2009). Plant polyphenols as dietary antioxidants in human health and disease. Oxid. Med. Cell. Longev. 2, 270-278.

Park, L.J., Ju, S.M., Song, H.Y., Lee, J.A., Yang, M.Y., Kang, Y.H., Kwon, H.J., Kim, T.Y., Choi, S.Y., and Park, J. (2006). The enhanced monocyte adhesiveness after UVB exposure requires ROS and NF-kappaB signaling in human keratinocyte. J. Biochem. Mol Biol. 39, 618-625.

Park, E., Lee, N.H., Baik, J.S., and Jee, Y. (2008). Elaeocarpus sylvestris modulates gamma-ray-induced immunosuppression in mice: implications in radioprotection. Phytother. Res. 22, 1046-1051.

Siomek, A. (2012). NF-κB signaling pathway and free radical impact. Acta. Biochim. Pol. 59, 323-331.

Svobodová, A., Psotová J., and Walterová D. (2003). Natural phenolics in the prevention of UV-induced skin damage. A review. Biomed. Pap. Med. Fac. Univ. Palacky Olomouc Czech. Repub. 147, 137-145.

Svobodova, A., Walterova, D., and Vostalova, J. (2006). Ultraviolet light induced alteration to the skin. Biomed. Pap. Med. Fac. Univ. Palacky Olomouc Czech. Repub. 150, 25-38.

Uitto, J. Understanding premature skin aging. (1997). N. Engl. J. Med. 337, 1463-1465.

Wagener F.A., Carels, C.E., and Lundvig, D.M. (2013). Targeting the redox balance in inflammatory skin conditions. Int. J. Mol. Sci. 14, 9126-9167.

Wang, S., Uchi, H., Hayashida, S., Urabe, K., Moroi, Y., and Furue, M. (2009). Differential expression of phosphorylated extracellular signal-regulated kinase 1/2, phosphorylated p38 mitogen-activated protein kinase and nuclear factor-kappaB p105/p50 in chronic inflammatory skin diseases. J. Dermatol. 36, 534-540.

Yaar, M., and Gilchrest, B.A. (2007). Photoageing: mechanism, prevention and therapy. Br. J. Dermatol. 157, 874-887.

Yagura, T., Makita, K., Yamamoto, H., Menck, C.F., and Schuch, A.P. (2011). Biological sensor for solar ultraviolet radiation. Sensors (Basel) 11, 4277-4294.

Yu, W.S., Jeong, S.J., Kim, J.H., Lee, H.J., Song, H.S., Kim, M.S., Ko, E., Lee, H.J., Khil, J.H., Jang, H.J., et al. (2011). The genome-wide expression profile of 1,2,3,4,6-penta-O-galloyl-β-D-glucose-treated MDA-MB-231 breast cancer cells: molecular target on cancer metabolism. Mol. Cells 32, 123-132.

Zhang, J., Li, L., Kim, S.H., Hagerman, A.E., and Lü, J. (2009). Anti-cancer, anti-diabetic and other pharmacologic and biological activities of penta-galloyl-glucose. Pharm. Res. 26, 2066-2080.